ORIGINAL PAPER

Biological and clinical heterogeneity of *MYCN*-amplified medulloblastoma

Andrey Korshunov · Marc Remke · Marcel Kool · Thomas Hielscher · Paul A. Northcott ·
Dan Williamson · Elke Pfaff · Hendrik Witt · David T. W. Jones · Marina Ryzhova ·
Yoon-Jae Cho · Andrea Wittmann · Axel Benner · William A. Weiss · Andreas von Deimling ·
Wolfram Scheurlen · Andreas E. Kulozik · Steven C. Clifford · V. Peter Collins ·
Frank Westermann · Michael D. Taylor · Peter Lichter · Stefan M. Pfister

Abstract Focal high-level amplifications of *MYC* (*or MYCC*) define a subset of high-risk medulloblastoma patients. However, the prognostic role of *MYCN* oncogene amplification remains unresolved. We aimed to evaluate the prognostic value of this alteration alone and in combination with biological modifiers in 67 pediatric medulloblastomas with *MYCN* amplification (*MYCN*-MB). Twenty-one *MYCN*-MB were examined using gene expression profiling and array-CGH, whereas for 46 tumors immunohistochemical analysis and FISH were performed. All 67 tumors were further subjected to mutational analyses. We compared molecular, clinical, and prognostic characteristics both within biological *MYCN*-MB groups and with non-amplified tumors. Transcriptomic analysis revealed SHH-driven tumorigenesis in a subset of *MYCN*-

A. Korshunov · A. von Deimling
Department of Neuropathology, University of Heidelberg,
Heidelberg, Germany

A. Korshunov · A. von Deimling
Clinical Cooperation Unit Neuropathology, German Cancer
Research Center, Heidelberg, Germany

M. Remke · M. Kool · E. Pfaff · H. Witt ·
D. T. W. Jones · A. Wittmann · P. Lichter · S. M. Pfister
Division Molecular Genetics, German Cancer Research Center,
Heidelberg, Germany

M. Remke · H. Witt · A. E. Kulozik · S. M. Pfister
Department of Pediatric Oncology, Hematology
and Immunology, University of Heidelberg, Heidelberg,
Germany

T. Hielscher · A. Benner
Division Biostatistics, German Cancer Research Center,
Heidelberg, Germany

P. A. Northcott · M. D. Taylor
Program in Developmental and Stem Cell Biology,
Division of Neurosurgery, Arthur and Sonia Labatt Brain
Tumour Research Centre, Hospital for Sick Children,
University of Toronto, Toronto, Canada

D. Williamson · S. C. Clifford
Northern Institute for Cancer Research, Newcastle University,
Newcastle upon Tyne, UK

M. Ryzhova
NN Burdenko Neurosurgical Institute, Moscow, Russia

Y.-J. Cho
Children's Hospital Boston, Boston, USA

W. A. Weiss
Departments of Neurology, Pediatrics, and Neurological
Surgery, UCSF, San Francisco, USA

W. Scheurlen
Cnopf'sche Kinderklinik, Nürnberg Children's Hospital,
Nürnberg, Germany

V. Peter Collins
Division of Molecular Histopathology,
Department of Pathology, University of Cambridge,
Cambridge, UK

F. Westermann
Division Tumor Genetics, German Cancer Research Center,
Heidelberg, Germany

S. M. Pfister (✉)
Im Neuenheimer Feld 280, 69120 Heidelberg, Germany
e-mail: s.pfister@dkfz.de

MBs indicating a biological dichotomy of *MYCN*-MB. Activation of SHH was accompanied by variant-specific cytogenetic aberrations including deletion of 9q in SHH tumors. Non-SHH MB were associated with gain of 7q and isochromosome 17q/17q gain. Among clinically relevant variables, SHH subtype and 10q loss for non-SHH tumors comprised the most powerful markers of favorable prognosis in *MYCN*-MB. In conclusion, we demonstrate considerable heterogeneity within *MYCN*-MB in terms of genetics, tumor biology, and clinical outcome. Thus, assessment of disease group and 10q copy-number status may improve risk stratification of this group and may delineate *MYCN*-MB with the same dismal prognosis as *MYC* amplified tumors. Furthermore, based on the enrichment of *MYCN* and *GLI2* amplifications in SHH-driven medulloblastoma, amplification of these downstream signaling intermediates should be taken into account before a patient is enrolled into a clinical trial using a smoothened inhibitor.

Introduction

Medulloblastoma (MB) is a clinically and biologically highly heterogeneous disease [6, 11, 12, 20, 30, 31, 35–37]. Staging systems for MB based on clinical parameters such as metastatic stage, patient age, extent of surgery, and pathological variants are still commonly used in clinical practice, although they do not sufficiently reflect the true heterogeneous nature of these neoplasms [7, 10, 11, 13, 16, 23, 35, 36, 41, 46]. Integrated molecular information including DNA copy-number and gene expression profiling studies have indicated that MB comprises distinct molecular variants that disclose significant differences in their patient demographics and clinical outcomes [6, 12, 20, 23, 36]. Amplification of *MYC* family oncogenes appears to be pivotal for tumor biology and clinical behavior in up to 15% of pediatric cases [9, 11, 30, 35, 36]. It has been recognized that focal high-level amplification of the *MYC* (*MYCC*) locus at 8q24 was significantly associated with poor clinical outcome and this has been confirmed in various independent series [1, 6, 11, 12, 35, 48].

However, the prognostic significance of *MYCN* oncogene amplification (2p24) is less striking and remains to be investigated in a large patient cohort with this alteration. Our preliminary work revealed that *MYCN* amplification was generally associated with a dismal prognosis [35]. When comparing the prognostic value of *MYCN* and *MYC* amplification in MB separately, *MYCN*-amplified MB (*MYCN*-MB) patients appeared to be clinically more

heterogeneous than those with tumors carrying a *MYC* amplification [35]. In contrast, other reports did not find any prognostic significance for *MYCN* amplification [1, 7, 11, 12, 16, 41]. Moreover, *MYCN*-MB display considerable molecular heterogeneity. Recent gene expression profiling studies demonstrated that *MYCN*-MB could be identified in various molecular disease variants, including SHH-driven MB, and group D tumors [30]. This is in contrast to *MYC* amplification, which constitutes a hallmark alteration almost exclusively found in group C tumors [12, 30, 39]. Additionally, in contrast to other frequently amplified MB oncogenes, *MYCN* amplification was identified as an acquired secondary aberration in recurrent tumors and was also found to be absent in metastases from *MYCN*-MB, which suggests that *MYCN* amplification comprises a late rather than a tumor-initiating event [21].

In the present study, we identified two distinct subgroups within *MYCN*-MB based on the integration of transcriptional, genetic and cytogenetic data. This additional knowledge will help to separate *MYCN*-MB patients with dismal prognosis from patients who have a high chance of being cured, and thereby further improve current molecular-based risk stratification algorithms.

Materials and methods

Tumor material and patient characteristics

A set of 67 primary *MYCN*-MB samples previously detected by array-CGH and/or FISH was designated for further molecular analyses. For 21 cases, sufficient amounts of high quality RNA and DNA were available to conduct gene expression profiling and array-CGH, respectively. The remaining cases were studied by immunohistochemistry and FISH. Clinical and histological data for the two patient cohorts are outlined in Supplementary Table 1. All tumor specimens were serially collected in accordance with the Ethics Review Boards of the NN Burdenko Neurosurgical Institute (Moscow, Russia), Würzburg University Hospital (Würzburg, Germany), Academic Medical Center (Amsterdam, Netherlands), Northern Institute for Cancer Research (Newcastle upon Tyne, UK), and Hospital for Sick Children (Toronto, Canada). Follow-up data were available for 50 patients which were treated in multicenter studies according to the national study protocols during the period from 1995 to 2010. Among them, 45 patients were treated according to the standardized therapy protocols of the German HIT study group as described previously [35]. Details of the postoperative treatment for remaining five patients are unknown.

DNA copy-number and expression profiling analysis

DNA copy-number and expression array data were generated from banked frozen tissue using an in-house array-CGH and the 4×44 K feature Agilent Whole Human Genome Oligo Microarray (GEO accession no. GPL6480), respectively, and analyzed as described [22, 34, 35]. Datasets will be available at the NCBI Gene Expression Omnibus (GEO) database upon publication (GSE30530).

Fluorescence in situ hybridization (FISH)

Multicolor interphase fluorescence in situ hybridization (FISH) analysis for *MYCN* (2p24), *GLI1* (12q13), *GLI2* (2q14), 9q22, 10q23, 17p13.3, and 17q21 was performed as described [22, 34, 35].

TP53 mutational analysis

The entire coding sequence of TP53 was analyzed in all 67 cases as previously described [34].

Immunohistochemistry (IHC)

Antibodies against the following antigens were used: β-catenin (BD Transduction Laboratories; ab610154; 1:100; WNT marker), secreted frizzled-related protein 1 (SFRP1; Abcam; ab4193; 1:2000; SHH marker), atrion-atriuretic peptide receptor C (NPR3; Abcam; ab37617; 1:200, group C marker), and potassium voltage-gated channel 1 (KCNA1; Abcam; ab32433; 1:2000; group D marker). Immunostaining was performed, evaluated, and scored for ß-catenin, SFRP1, NPR3, and KCNA1 as published [30, 40]. In addition, IHC was performed and evaluated for GRB2-associated-binding protein 1 (GAB1; Abcam; ab27439; 1:50) which has been previously proposed as a surrogate SHH marker [11].

Biostatistics and bioinformatics

Missing gene expression values were imputed using nearest neighbor method. Unsupervised hierarchical clustering (HCL) was performed using complete linkage and dissimilarity based on Euclidian distances. Cluster reliability was assessed using a bootstrap-based approach [44] which gives approximately unbiased probabilities. Goeman's global test with logistic regression model was used to descriptively rank individual transcripts in their influence on cluster definition [14]. Principal component analysis (PCA) and semi non-negative matrix factorization (NMF) were applied as additional class discovery approaches. Semi-NMF was chosen to include two components based on the cophenetic correlation coefficient. The algorithm [24] as implemented by Qi et al. [38]. was used. The consensus matrix of multiple runs was used to assess stability of semi NMF results.

Clones exceeding 25% missing values were removed from array-CGH analysis. Remaining missing values were imputed based on the lowess method. Gains and losses were deduced using a scaling factor of 2 and median averaged by chromosome arm.

The Kaplan–Meier method was used to estimate distribution of survival times. The prognostic value of groups was compared with log-rank test and Cox PH regression model. Prediction accuracy was assessed with the Brier score over time, using $0.632 +$ bootstrap estimates to avoid overfitting bias [15]. Brier scores provide a measure for the average squared deviation between predicted probabilities for a set of events and their outcomes, thus a lower score indicates higher accuracy. Groups were compared for differences in clinicopathological parameters using Fisher's exact test. *p* values below or equal to 0.05 were considered statistically significant. All analyses were carried out with R 2.12/Bioconductor 2.7 using add-on packages NMF, pvclust, aCGH and pec.

An ARACNE network was calculated using the ARACNE2 stand-alone linux executable [26, 27]. Hundred bootstraps were created using 77 primary MB expression profiles centered and filtered to remove non-varying probes. Estimated interactions with a probability of $p < 1e-8$ were retained. Gene set enrichment analysis (GSEA) was performed using the stand-alone tool (Broad Institute) and the MSigDB C2.V3 Gene set collection. Genes were pre-ranked according to their corrected *t* value as calculated using the R package limma. A geneset enrichment map was produced using Cytoscape 2.8.1 and the EnrichmentMapv1.1 plugin. The Jaccard statistic was used to calculate significant overlap in gene sets and $p < 0.01$ and $q < 0.1$ chosen as a moderately permissive cutoff.

Results

Transcriptomic profiling of *MYCN*-amplified medulloblastomas (*MYCN*-MB)

Genome-wide gene expression analysis including non-*MYCN*-MB ($n = 56$; as previously reported [39]) showed *MYCN*-MB ($n = 21$) to be enriched in the SHH and group D variants, with only one case lying outside of these two groups (Supplementary Figure 1). To understand the biological differences between subgroups within *MYCN*-MB samples, this cohort was subsequently analyzed separately. Clinicopathological and molecular characteristics of this cohort are summarized in Supplementary Table 1.

Unsupervised hierarchical cluster analysis (HCL) delineated two distinct sample clusters within *MYCN*-MB using a gene list including 300 high-variance transcripts (Fig. 1a). Bootstrap analysis of the clustering data indicated high confidence for these two groups (≥95%). Semi NMF using the same 300 transcripts confirmed the existence of two stable groups with identical sample allocation (Fig. 1b) [5]. The distinction of two stable clusters was further underlined by PCA, which revealed reliable and clear separation of the two groups using the same gene list as for HCL or NMF (Fig. 1c).

To delineate characteristic signaling patterns for each of the clusters, we performed pathway annotation using Ingenuity. Cluster 1 was enriched with gene sets associated with SHH signaling (5 cases, SHH), whereas Cluster 2 tumors were characterized by over expression of genes involved in synaptogenesis, neuronal differentiation and glutamatergic receptors (16 cases, non-SHH). Subgroup-specific signature gene sets of each cluster are supplied in Supplementary Table 2. Due to the large overlap of marker genes and deregulated pathways in non-SHH tumors with previously reported variants in pediatric MB, most of these tumors ($n = 14$) were classified as "group D" and only two tumors were allocated to "group C" according to the proposed group denomination [30, 39]. These transcriptomic distinctions within *MYCN*-MB were further underlined by specific alterations including a significantly higher frequency of 9q loss ($p = 0.03$), and significantly lower frequencies of 17p13.loss/17q21gain ($p = 0.004$), and 7q gain ($p = 0.001$) within SHH *MYCN*-MB (Fig. 1d). Similar distribution of cytogenetic aberrations for SHH and non-SHH tumors were observed in the 56 MB without *MYCN* amplification.

Network analyses and candidate genes

A bootstrapped ARACNE network analysis was performed using all primary MB expression data to reverse engineer interactions between genes. This analysis revealed cooperating effects of MYCN- and GLI2-driven transcriptional signatures (Supplementary Figure 2A). Similar transcript levels of *GLI2* were observed in all SHH-driven tumors, whereas *MYCN* expression was elevated in SHH MB compared to non-SHH MB. Apparently *MYCN* amplification is the key determinant of *MYCN* upregulation and results in high expression regardless of subtype (Supplementary Figure 2B). Taken as a whole, this suggests that the action of SHH pathway activation in MB is mediated to some extent through MYCN but that *MYCN* amplification leads to significantly higher *MYCN* transcript levels. GSEA revealed significant overrepresentation of "nuclear transport" and "mitotic cell cycle/G2-M" in tumors with *MYCN* amplification (Fig. 2a). Notably, SHH *MYCN*-MB demonstrated

overrepresentation of gene sets associated with "RNA processing", "telomerase maintenance", and "protein translation" in addition to the expected presence of "Hedgehog signaling pathway", whereas "membrane transport" was associated with non-SHH *MYCN*-MB gene sets (Fig. 2b).

Immunohistochemical analysis confirmed two distinct groups of *MYCN*-MB

We performed immunostaining of variant-specific marker genes for formalin-fixed paraffin-embedded (FFPE) samples from 46 *MYCN*-MB following a recently proposed stratification model using four commercially available antibodies [30, 40]. *MYCN* amplification in these cases was detected by FISH.

All 46 tumors stained positive for only a single marker. Immunopositivity for SFRP1, indicative of SHH activation, was found in 21 of 46 *MYCN*-MB. Moreover, 38 tumors from the FFPE set (16 SFRP1-positive and 22 SFRP1-negative) were also available for GAB1 IHC analysis as an alternative marker for SHH activation [11]. We found that 15/16 (94%) SFPR1-positive tumors were also positive for GAB1. Conversely, all of the SFRP1-negative *MYCN*-MB were also negative for GAB1. The high overlap of both immunostaining approaches underlines the practical value of these assays to detect SHH pathway activation. In line with the GEP results, the remaining 25 (non-SHH) tumors showed positive marker staining predominantly for group D (23 positive for KCNA1), and rarely for group C (2 positive for NPR3) (Fig. 3). In addition, we confirmed the reliability of our immunohistochemical findings, applying FFPE samples of 11 tumors included in expression profiling cohort. Notably, six of them were analyzed in an independent laboratory (Burdenko Institute). All three tumors allocated to SHH GEP group showed only SFRP1 immunopositivity, whereas the remaining eight tumors from group D were positive for KCNA1 exclusively (see Fig. 3).

Clinical and cytogenetic differences between molecular groups of *MYCN*-MB

Combining both transcriptome and immunostaining data, 38% of *MYCN*-MB showed SHH pathway activation, whereas the remaining 62% of cases belonged to non-SHH groups (predominantly group D). Differences regarding clinicopathological (Fig. 4) and molecular (Fig. 5) variables between the variants of *MYCN*-MB could be identified. As expected, a higher incidence of SHH tumors was observed in infants compared to their counterparts [6, 20, 30, 39]. Non-SHH tumors showed a male preponderance (67 vs. 33%), while in SHH-driven tumors gender distribution was equal (50 vs. 50%). Metastatic dissemination at diagnosis (M1-3)
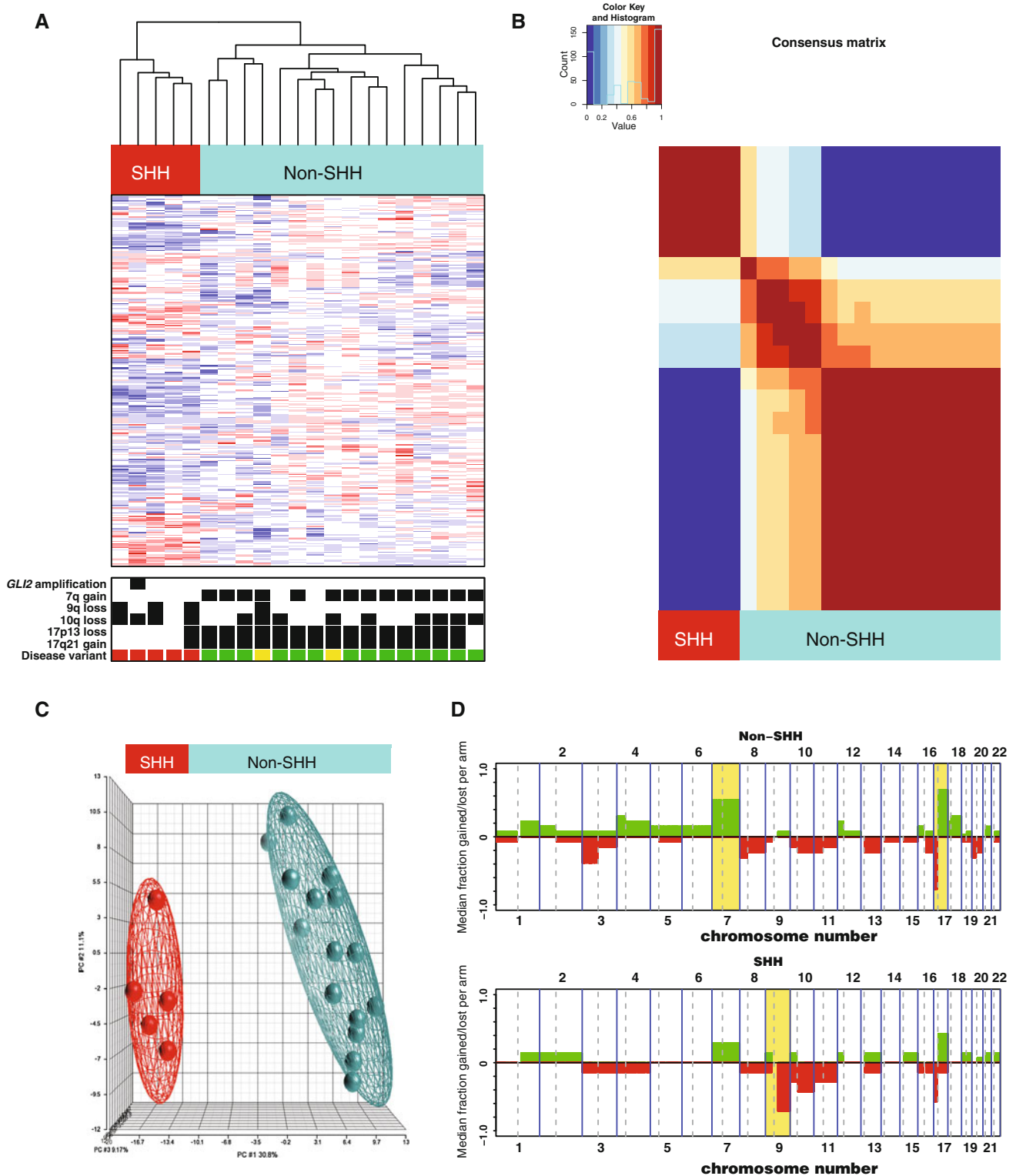
Fig. 1 (a) Unsupervised hierarchical clustering from 21 primary *MYCN*-amplified medulloblastomas using 300 genes with high standard deviation. Molecular characteristics [*GLI2* amplification; gain of chromosome 7, loss of 9q, 10q, and 17p; gain of 17q; disease variant denominations: SHH (*red*), group C (*yellow*), and group D (*green*)] of the study population are shown below the dendrogram. Molecular alteration present (*black*). (b) Semi non-negative matrix factorization (NMF) of the primary tumors used in (a) demonstrates two groups exactly recapitulating the consensus HCL subtype classification. (c) Principle component analysis (PCA) of the primary tumors described in (a) using 300 high SD genes. (d) Frequency plot of DNA copy-number alterations non-SHH and SHH *MYCN*-MB delineates group-specific genomic imbalances (indicated by *yellow* highlight)

Fig. 2 Processes differentially regulated between **a** *MYCN*-amplified and non-*MYCN*-amplified medulloblastoma, **b** SHH and non-SHH *MYCN*-amplified medulloblastoma. Enrichment map representations of GSEA results. Node color and shading intensity represent the statistical significance of enrichment of a particular gene set. *Edges* represent significant overlap between gene sets
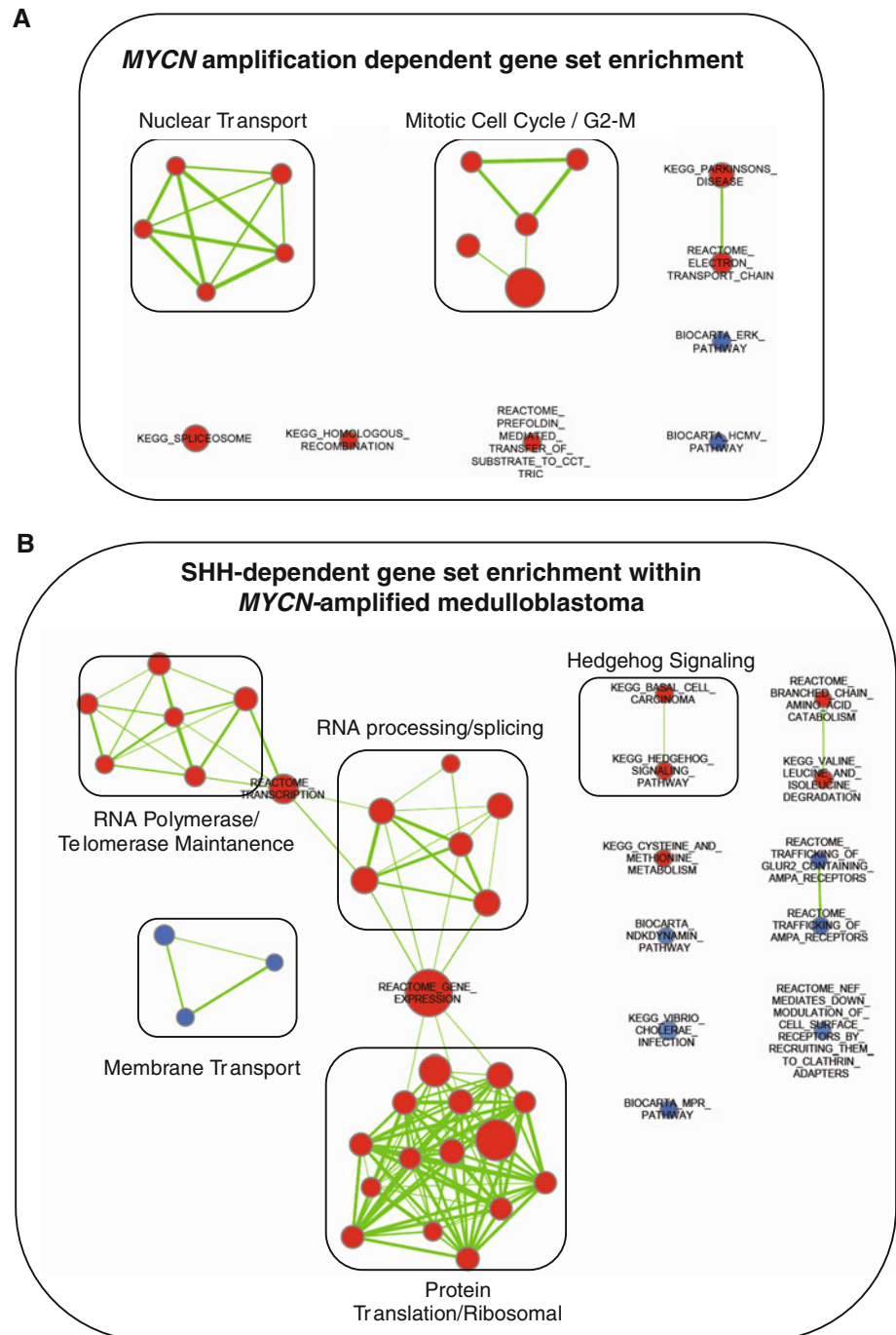
was predominantly identified in non-SHH *MYCN*-MB (65 vs. 11% for SHH tumors; $p < 0.001$). Histology was significantly associated with grouping of *MYCN*-MB according to SHH activation ($p < 0.001$): Classic histology was more common in non-SHH tumors (74 vs. 36% for SHH), whereas all seven tumors with desmoplastic histology were of the SHH variant. Large cell/anaplastic histology (LCA) was rather evenly distributed among both molecular groups (27 and 38%, respectively). Losses of 9q and 10q were more frequent in SHH tumors [60 vs. 5% ($p < 0.0001$) and 84 vs.

32% ($p < 0.0001$), respectively], whereas isochromosome 17 (characterized by 17p loss and concomitant 17q gain), or isolated 17q gain, and gain of 7q were significantly associated with non-SHH tumors (95 vs. 24%; $p < 0.0001$ and 61 vs. 16%; $p < 0.001$, respectively). Furthermore, almost all tumors with co-amplification of *MYCN*, and *GLI1/2* oncogenes ($n = 13$) were of the SHH variant [12/13 (92%)], with only one case in group D. FISH analysis of ten of these cases with accessible FFPE material revealed co-amplifications of these genomic loci in the same tumor nuclei in nine cases and
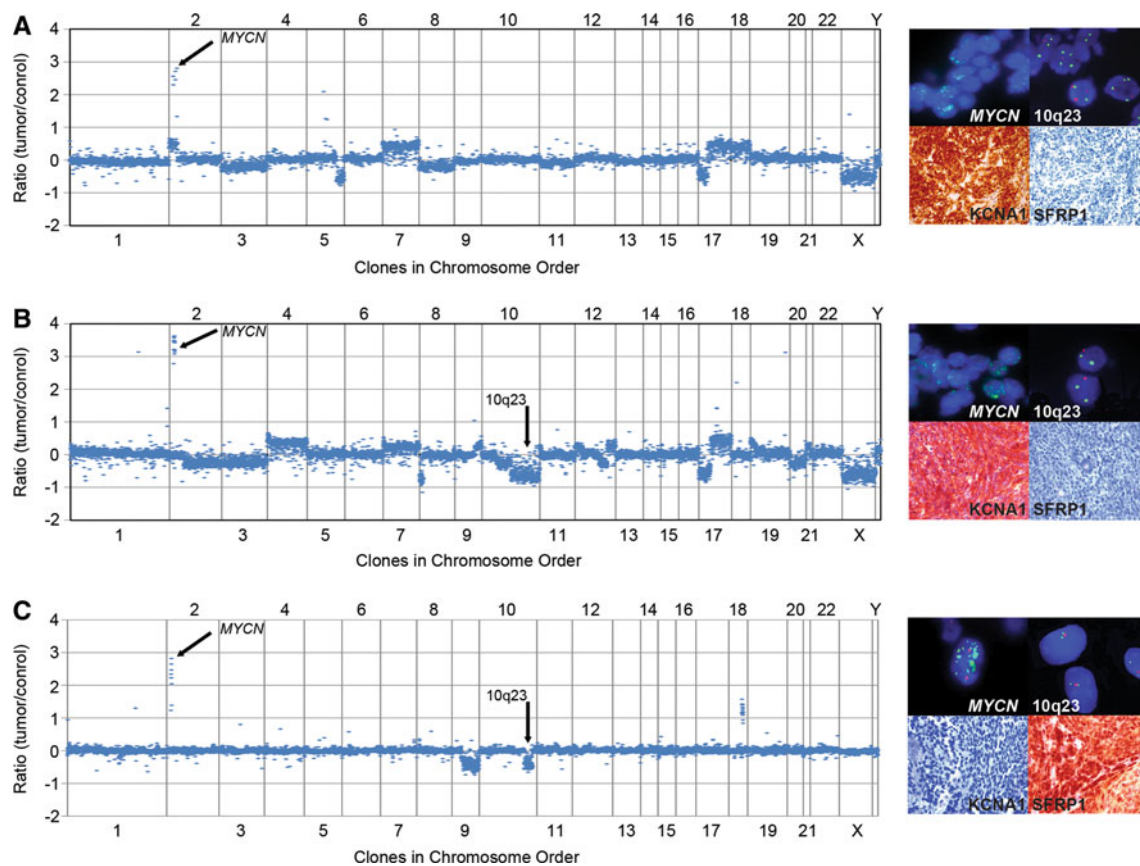
Fig. 3 Characteristic genomic aberrations and protein expression patterns in distinct molecular subgroups of *MYCN*-amplified medulloblastomas (*MYCN*-MB). **a** Array-based comparative genomic hybridization (aCGH) profile, fluorescence in situ hybridization (FISH) findings, and immunohistochemical staining patterns in non-SHH *MYCN*-MB with balanced 10q, and expression of KCNA1 (group D marker). **b** Representative aCGH profile, FISH validation, and immunostaining in non-SHH *MYCN*-MB with loss of 10q, and expression of KCNA1 (group D marker). **c** Representative aCGH profile, FISH validation, and immunostaining in SHH *MYCN*-MB with loss of 10q, and expression of SFRP1 (SHH marker)

one sample showed *MYCN* and *GLI2* amplifications in distinct subpopulations of tumor cells (data not shown). In addition, almost half of SHH-driven *MYCN*-MB (11/25 = 44%) also harbored a *TP53* mutation, whereas only one of the 40 tumors from the non-SHH subset showed this genetic alteration. Comparisons between GEP and FFPE cohorts revealed a similar distribution of these molecular aberrations among SHH and non-SHH tumors.

Taken together, distinct molecular signatures including copy-number aberrations of chromosomes 7, 9q, and 17, focal amplification of *GLI1* or *GLI2*, and *TP53* mutation suggest important differences regarding the underlying tumorigenesis. Thus, we hypothesized that molecular characteristics may in addition define prognostic groups.

Molecular prognosticators in *MYCN*-MB

We tested prognostic associations in a large *MYCN*-MB patient cohort with follow-up data available for 50 patients with 19 SHH and 31 non-SHH tumors among them. Tumor recurrence was identified in 29 patients (58%) and 24

(48%) of those died during follow-up. Five-year progression-free survival (PFS), and 5-year overall survival (OS) were 39 and 47%, respectively. A univariable Cox PH model showed that none of the clinical variables examined reached statistical significance for either OS or PFS (Tables 1, 2). Surprisingly, LCA histology was not significantly associated with outcome in *MYCN*-MB, whereas desmoplastic/extensive nodularity (MBEN) histology was linked to favorable OS ($p = 0.05$). Among molecular variables, only SHH variant and 10q loss were significantly associated with both favorable PFS and OS (Tables 1, 2; both $p < 0.01$).

With respect to OS in the entire *MYCN*-MB patient cohort, amplifications of the *GLI1/2* oncogenes were also significantly associated with favorable outcomes ($p = 0.03$), whereas 17q gain showed a significant association with adverse prognosis ($p = 0.02$). When separately analyzing the 31 non-SHH tumors, only 10q loss remained a significant prognostic factor: only one out of seven patients with a tumor carrying this aberration died 94 months after the operation. We observed no significant

Fig. 4 Clinical characteristics of *MYCN*-amplified medulloblastomas according to SHH activation. Clinical variables include **a** age groups (<3, 3–5, 6–10, 11–18, >18), **b** gender (female, male), **c** histology [classic, large cell/anaplastic (LCA), desmoplastic/extensive nodularity (MBEN)], **d** M-Stage (M0, M1-3)
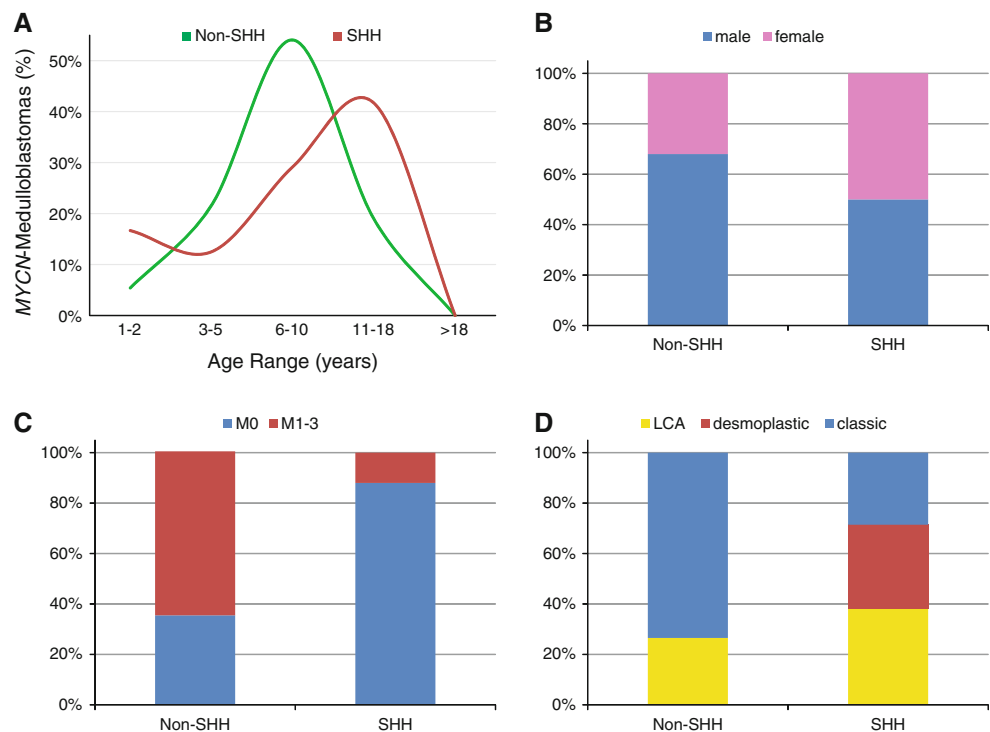
differences in OS between seven non-SHH tumors with 10q loss and 19 SHH-driven MB ($p = 0.50$). In addition, survival differences in SHH tumors depending on 10q loss could not be calculated since only two of these 19 tumors did not show this alteration.

We additionally performed survival analysis within the cohort of 77 MB with GEP data. Among them, *MYCN*-MB were significantly associated with inferior outcome compared to non *MYCN*-MB ($p = 0.01$), whereas prognosis for the whole cohort of SHH tumors showed a trend to be better than in non-SHH MB ($p = 0.08$, not shown). When we evaluated survival for SHH and non-SHH MB separately, we found that SHH-driven tumors were associated with a comparable outcome regarding OS and PFS independent of the presence of *MYCN* amplification (Supplementary Figure 3). In contrast, non-SHH *MYCN*-MB were associated with significantly inferior outcome compared to non-SHH tumors without *MYCN* amplification ($p = 0.004$; Supplementary Fig. 4).

The multivariable Cox proportional hazards model was applied to assess the role of molecular markers to predict OS and PFS. Importantly, only 10q loss ($p < 0.01$ for OS and PFS), was found to be an independent significant predictor for both OS and PFS (Supplementary Table 4A/B).

Revised molecular risk stratification of *MYCN*-MB

Due to the significant molecular heterogeneity within the *MYCN*-MB, and the clear advantage of molecular markers over all available clinical markers, the final goal of our work was the proposal of a clinically useful strategy for risk assessment of *MYCN*-MB. Based on our aforementioned results, we propose a hierarchical molecular stratification scheme for *MYCN*-MB comprising two relatively equal groups (Fig. 6; $p < 0.001$): (1) 24 non-SHH *MYCN*-MB with balanced 10q (5-year OS = 6%; 48% of patients), (2) all 19 SHH *MYCN*-MB (regardless of 10q status) plus seven non-SHH *MYCN*-MB with 10q loss (5-year OS = 83%, 52% of patients). Notably, the proposed hierarchical molecular stratification scheme considerably improves the prediction accuracy (Brier score over time; Fig. 6).

Discussion

The *MYCN* oncogene belongs to the MYC family of transcription factors [45]. It is primarily expressed during normal embryogenesis and is thought to be critical in brain development [18, 19, 32, 45]. MYCN is a pivotal regulator of proliferation and apoptosis (reviewed in [45, 47]). Due to its orchestrating role of central cellular functions, deregulation of MYCN constitutes a commonly observed trigger for tumor development in combination with other oncogenic events [19, 29, 45]. *MYCN* oncogene amplification is centrally important in the pathogenesis of peripheral neuroblastomas [28]. In this childhood malignancy, as MB derived from the neuroectoderm, *MYCN*

Fig. 5 Molecular characterization of 67 primary *MYCN*-amplified medulloblastomas (*MYCN*-MB) according to SHH activation. *Bar charts* showing the frequency of 9q loss (**a**) and 10q loss (**b**) in non-SHH and SHH *MYCN*-MB. Relative frequency of isochromosome i(17q) formation or isolated 17q gain (**c**) and chromosome 7q gain (**d**). Presence of focal amplifications of *GLI1* or *GLI2* (**e**) or *TP53* mutational status (**f**)
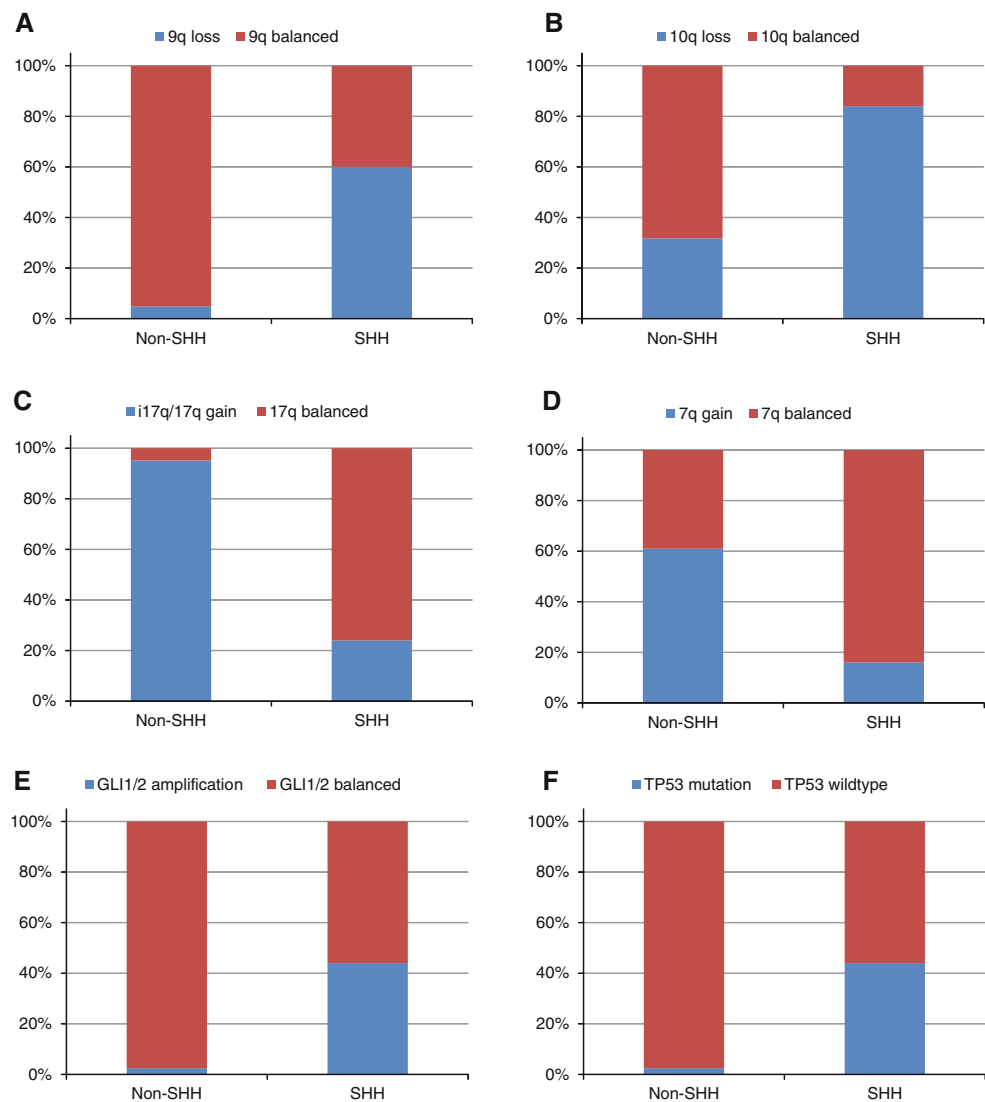
amplification is present in 20% of tumors [42]. Further, it defines a patient cohort with unfavorable prognosis and as such was successfully implemented as a stratification marker in multicenter clinical trials [33, 42]. Interestingly, *MYCN* amplification in neuroblastoma shows a remarkable association with 17q gain [4].

In MB, *MYCN* amplification has been identified as a recurrent focal amplification in around 3% of cases [10, 36]. However, its prognostic value remains controversial. Earlier studies evaluated small *MYCN*-MB cohorts only, which likely explains the contradictory results regarding its value as a prognostic biomarker [1, 7, 8, 11, 12, 16, 23, 35, 41]. In this study, we analyzed a large cohort of 67 *MYCN*-MB and explored whether molecular data could be translated into a prognostic model for further stratification of these tumors. Clinical factors including LCA histology showed no prognostic significance regardless of the impressive representation (30%) of LCA tumors

among *MYCN*-MB. This intriguing observation might be partly explained by the relatively high incidence of LCA histology in the clinically more favorable SHH *MYCN*-MB.

Our current study demonstrated a strong molecular heterogeneity of *MYCN*-MB. Both transcriptome analyses and immunoprofiling identified a distinct subset of *MYCN*-MB with aberrant SHH activation. Importantly, SHH-driven tumors revealed a significantly better OS and PFS. A recent report by Ellison et al. [11] also detected two similar subgroups among 12 *MYCN*-MB. In contrast to our study, SHH tumors were reported to be associated with inferior outcome in that study. Due to the high concordance of immunostaining for SFRP1 and GAB1, the survival discrepancy may be explained by differences in terms of (1) size of the investigated study cohort, and/or (2) the treatment modalities (PNET3 protocol compared to HIT protocol in our cohort).

Fig. 6 Kaplan–Meier plot of estimated overall survival (*left panel*) and progression-free (*right panel*) time distributions. The number of patients under risk is indicated for time increments of 24 months. **a** Kaplan–Meier plot for overall survival of patients with *MYCN*-amplified medulloblastomas (*MYCN*-MB) according to SHH grouping (*red line*), non-SHH tumors with 10q loss (*blue line*), and non-SHH *MYCN*-MB with balanced 10q status (*green line*). **b** Kaplan–Meier plot for progression-free survival of patients with *MYCN*-MBs according to SHH grouping (*red line*), Non-SHH tumors with 10q loss (*blue line*), and non-SHH *MYCN*-MB with balanced 10q status (*green line*). **c** Cumulative prediction error of risk marker models in non-SHH tumors with balanced 10q vs. other *MYCN*-MB (*red line*). Brier score is calculated over time with ordinary Kaplan-Meier estimates being the reference (*black line*)
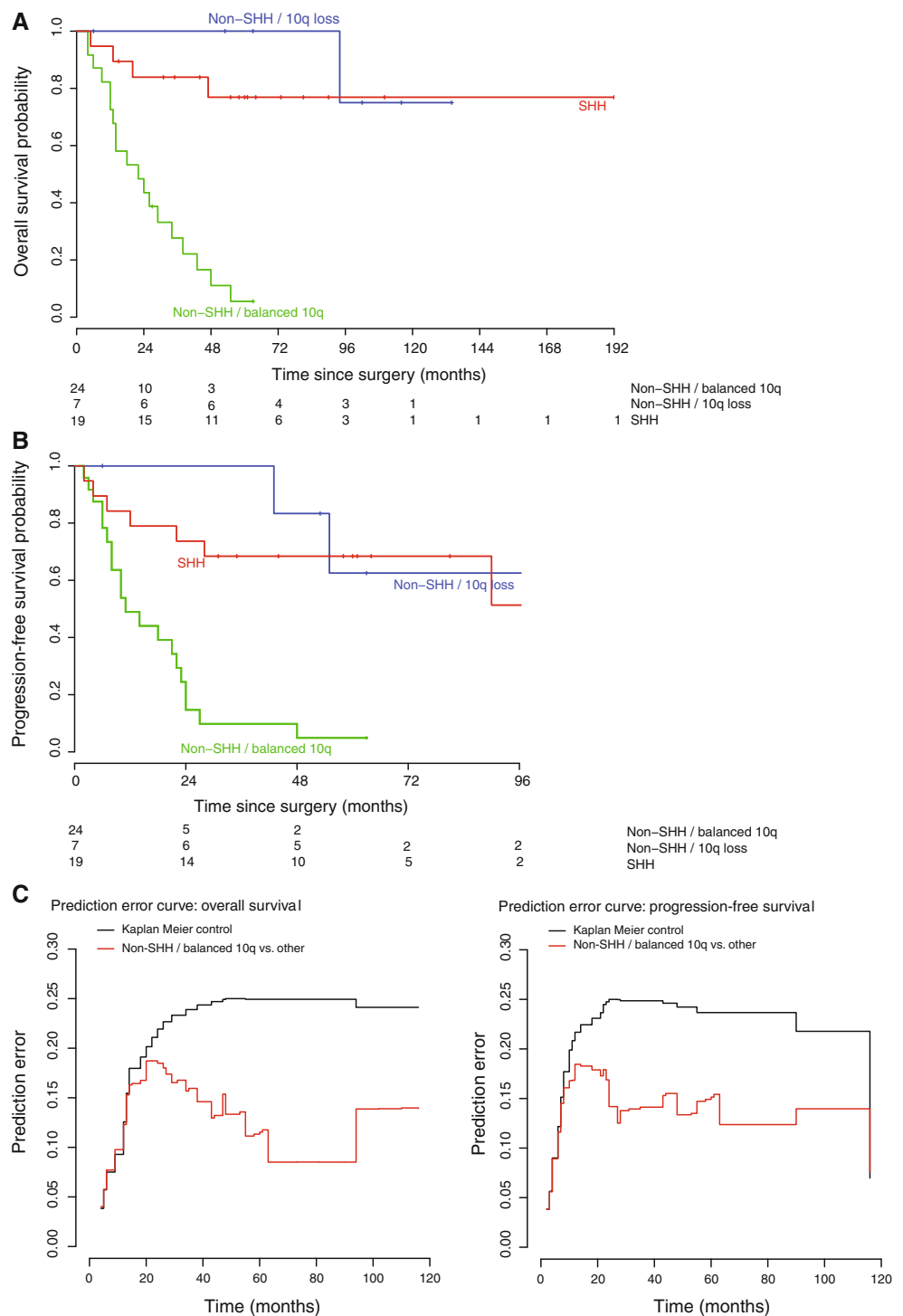
Notably, 10q loss was identified as the strongest independent predictor of favorable outcome in *MYCN*-MB. This aberration was found in the majority of SHH tumors (90%) and in approximately 25% of non-SHH MB. According to previous reports, 20% of MB harbor deletions on chromosome 10, the clinical relevance of which remains controversial [22, 30, 35, 43]. This aberration was reportedly not prognostic for pediatric MB but constituted a strong

biomarker for poor prognosis in adult tumors [22, 35]. It is unclear which biological mechanisms may underlie the prognostic distinctions between 10q deleted and balanced *MYCN*-MB. Comparisons of expression profiles showed that these cytogenetic groups could not be discriminated on the basis of their transcriptional programs (data not shown).

Strikingly, amplification of *GLI1/2* oncogenes was found to be a frequent event in SHH-driven *MYCN*-MB, thus

Table 1 Overall survival, univariate analysis

Variable	Hazard ratio	LCL	UCL	p value
Age				
<3 versus >3 years	0.82	0.24	2.78	0.75
Gender				
Male versus female	1.66	0.73	3.81	0.23
M stage				
M+ versus M0	1.93	0.86	4.33	0.11
Histology				
Desmoplastic/MBEN versus classic	0.14	0.02	1.03	0.05
LCA versus classic	0.52	0.19	1.41	0.20
Disease variant				
SHH versus non-SHH	0.21	0.07	0.63	<0.01
9q loss				
Yes versus no	0.41	0.14	1.20	0.10
10q loss				
Yes versus no	0.07	0.02	0.26	<0.01
i(17q)/17q gain				
Yes versus no	5.77	1.35	24.58	0.02
GLI1/2 amplification				
Yes versus no	0.20	0.05	0.87	0.03
TP53 mutation				
Yes versus no	0.42	0.13	1.42	0.16

Table 2 Progression-free survival, univariate analysis

Variable	Hazard ratio	LCL	UCL	p value
Age				
<3 versus >3 years	1.19	0.36	3.94	0.77
Gender				
Male versus female	2.15	0.99	4.68	0.05
M stage				
M+ versus M0	2.03	0.97	4.25	0.06
Histology				
Desmoplastic/MBEN versus classic	0.21	0.05	0.92	0.04
LCA versus classic	0.47	0.19	1.18	0.10
Disease variant				
SHH versus non-SHH	0.31	0.13	0.74	<0.01
9q loss				
Yes versus no	0.41	0.16	1.08	0.07
10q loss				
Yes versus no	0.15	0.062	0.37	<0.01
i(17q)/17q gain				
Yes versus no	2.16	0.87	5.33	0.09
GLI1/2 amplification				
Yes versus no	0.48	0.18	1.26	0.13
TP53 mutation				
Yes versus no	0.65	0.25	1.72	0.38

corroborating the previously published observation [6]. GLI2 and MYCN were frequently co-amplified in the same cells, suggesting a clonal origin of tumors bearing such co-amplifications. Importantly, treatment with SMO inhibitors will likely be ineffective for SHH-driven MB harboring MYCN/GLI amplifications, because these inhibitors target the SHH pathway upstream of MYCN and GLI2 [2, 3, 17, 25]. Further studies are warranted to identify the potential targets for therapeutic interventions in the heterogeneous cohort of pediatric MYCN-MB.

In conclusion, we identified two subgroups within MYCN-MB with distinct molecular abnormalities, clinical characteristics, and prognosis. At the time of diagnosis, SHH activation and 10q status can readily be determined in routine pathological laboratories by IHC and FISH. Variant-specific risk stratification approaches incorporating cytogenetic and subtype information may help to further individualize treatment intensities for the most common malignant brain tumor in childhood.

Conflict of interest The authors declare no conflicts of interest.

References

1. Aldosari N, Bigner SH, Burger PC, Becker L, Kepner JL, Friedman HS, McLendon RE (2002) MYCC and MYCN oncogene amplification in medulloblastoma. A fluorescence in situ hybridization study on paraffin sections from the Children's Oncology Group. Arch Pathol Lab Med 126(5):540–544
2. Beauchamp EM, Ringer L, Bulut G, Sajwan KP, Hall MD, Lee YC, Peaceman D, Ozdemirli M, Rodriguez O, Macdonald TJ, Albanese C, Toretsky JA, Uren A (2011) Arsenic trioxide inhibits human cancer cell growth and tumor development in mice by blocking Hedgehog/GLI pathway. J Clin Invest 121(1):148–160. doi:10.1172/JCI4287442874
3. Berman DM, Karhadkar SS, Hallahan AR, Pritchard JI, Eberhart CG, Watkins DN, Chen JK, Cooper MK, Taipale J, Olson JM, Beachy PA (2002) Medulloblastoma growth inhibition by hedgehog pathway blockade. Science 297(5586):1559–1561. doi:10.1126/science.1073733297/5586/1559
4. Bown N, Cotterill S, Łastowska M, O'Neill S, Pearson ADJ, Plantaz D, Meddeb M, Danglot G, Brinkschmidt C, Christiansen H, Laureys G, Nicholson J, Bernheim A, Betts DR, Vandesompele J, Van Roy N, Speleman F (1999) Gain of chromosome arm 17q and adverse outcome in patients with neuroblastoma. N Engl J Med 340(25):1954–1961. doi:10.1056/NEJM199906243402504
5. Brunet JP, Tamayo P, Golub TR, Mesirov JP (2004) Metagenes and molecular pattern discovery using matrix factorization. Proc

Natl Acad Sci USA 101(12):4164–4169. doi:10.1073/pnas.0308531101

6. Cho YJ, Tsherniak A, Tamayo P, Santagata S, Ligon A, Greulich H, Berhoukim R, Amani V, Goumnerova L, Eberhart CG, Lau CC, Olson JM, Gilbertson RJ, Gajjar A, Delattre O, Kool M, Ligon K, Meyerson M, Mesirov JP, Pomeroy SL (2011) Integrative genomic analysis of medulloblastoma identifies a molecular subgroup that drives poor clinical outcome. J Clin Oncol 29(11):1424–1430. doi:10.1200/JCO.2010.28.5148

7. Eberhart CG, Kratz J, Wang Y, Summers K, Stearns D, Cohen K, Dang CV, Burger PC (2004) Histopathological and molecular prognostic markers in medulloblastoma: c-myc, N-myc, TrkC, and anaplasia. J Neuropathol Exp Neurol 63(5):441–449

8. Eberhart CG, Kratz JE, Schuster A, Goldthwaite P, Cohen KJ, Perlman EJ, Burger PC (2002) Comparative genomic hybridization detects an increased number of chromosomal alterations in large cell/anaplastic medulloblastomas. Brain Pathol 12(1):36–44

9. Ellison D (2002) Classifying the medulloblastoma: insights from morphology and molecular genetics. Neuropathol Appl Neurobiol 28(4):257–282. doi:10.1046/j.1365-2990.2002.00419.x

10. Ellison DW (2010) Childhood medulloblastoma: novel approaches to the classification of a heterogeneous disease. Acta Neuropathol 120(3):305–316. doi:10.1007/s00401-010-0726-6

11. Ellison DW, Dalton J, Kocak M, Nicholson SL, Fraga C, Neale G, Kenney AM, Brat DJ, Perry A, Yong WH, Taylor RE, Bailey S, Clifford SC, Gilbertson RJ (2011) Medulloblastoma: clinicopathological correlates of SHH, WNT, and non-SHH/WNT molecular subgroups. Acta Neuropathol 121(3):381–396. doi:10.1007/s00401-011-0800-8

12. Ellison DW, Kocak M, Dalton J, Megahed H, Lusher ME, Ryan SL, Zhao W, Nicholson SL, Taylor RE, Bailey S, Clifford SC (2011) Definition of disease-risk stratification groups in childhood medulloblastoma using combined clinical, pathologic, and molecular variables. J Clin Oncol 29(11):1400–1407. doi:10.1200/JCO.2010.30.2810

13. Gajjar A, Hernan R, Kocak M, Fuller C, Lee Y, McKinnon PJ, Wallace D, Lau C, Chintagumpala M, Ashley DM, Kellie SJ, Kun L, Gilbertson RJ (2004) Clinical, histopathologic, and molecular markers of prognosis: toward a new disease risk stratification system for medulloblastoma. J Clin Oncol 22(6):984–993. doi:10.1200/JCO.2004.06.032

14. Goeman JJ, le Cessie S (2006) A goodness-of-fit test for multinomial logistic regression. Biometrics 62(4):980–985. doi:10.1111/j.1541-0420.2006.00581.x

15. Graf E, Schmoor C, Sauerbrei W, Schumacher M (1999) Assessment and comparison of prognostic classification schemes for survival data. Stat Med 18(17–18):2529–2545. doi:10.1002/(SICI)1097-0258(19990915/30)18:17/18<2529

16. Grotzer MA, von Hoff K, von Bueren AO, Shalaby T, Hartmann W, Warmuth-Metz M, Emser A, Kortmann RD, Kuehl J, Pietsch T, Rutkowski S (2007) Which clinical and biological tumor markers proved predictive in the prospective multicenter trial HIT'91–implications for investigating childhood medulloblastoma. Klin Padiatr 219(6):312–317. doi:10.1055/s-2007-985843

17. Katoh Y, Katoh M (2009) Hedgehog target genes: mechanisms of carcinogenesis induced by aberrant hedgehog signaling activation. Curr Mol Med 9(7):873–886

18. Kenney AM, Cole MD, Rowitch DH (2003) Nmyc upregulation by sonic hedgehog signaling promotes proliferation in developing cerebellar granule neuron precursors. Development 130(1):15–28

19. Kessler JD, Hasegawa H, Brun SN, Emmenegger BA, Yang ZJ, Dutton JW, Wang F, Wechsler-Reya RJ (2009) N-myc alters the fate of preneoplastic cells in a mouse model of medulloblastoma. Genes Dev 23(2):157–170. doi:10.1101/gad.1759909

20. Kool M, Koster J, Bunt J, Hasselt NE, Lakeman A, van Sluis P, Troost D, Meeteren NS, Caron HN, Cloos J, Mrsic A, Ylstra B, Grajkowska W, Hartmann W, Pietsch T, Ellison D, Clifford SC, Versteeg R (2008) Integrated genomics identifies five medulloblastoma subtypes with distinct genetic profiles, pathway signatures and clinicopathological features. PLoS One 3(8):e3088. doi:10.1371/journal.pone.0003088

21. Korshunov A, Benner A, Remke M, Lichter P, von Deimling A, Pfister S (2008) Accumulation of genomic aberrations during clinical progression of medulloblastoma. Acta Neuropathol 116(4):383–390. doi:10.1007/s00401-008-0422-y

22. Korshunov A, Remke M, Werft W, Benner A, Ryzhova M, Witt H, Sturm D, Wittmann A, Schottler A, Felsberg J, Reifenberger G, Rutkowski S, Scheurlen W, Kulozik AE, von Deimling A, Lichter P, Pfister SM (2010) Adult and pediatric medulloblastomas are genetically distinct and require different algorithms for molecular risk stratification. J Clin Oncol 28(18):3054–3060. doi:10.1200/JCO.2009.25.7121

23. Lamont JM, McManamy CS, Pearson AD, Clifford SC, Ellison DW (2004) Combined histopathological and molecular cytogenetic stratification of medulloblastoma patients. Clin Cancer Res 10(16):5482–5493. doi:10.1158/1078-0432.CCR-03-072110/16/5482

24. Li T, Ding C (2006) The relationships among various nonnegative matrix factorization methods for clustering. Paper presented at the Proceedings of Sixth International Conference on Data Mining

25. Low JA, de Sauvage FJ (2010) Clinical experience with Hedgehog pathway inhibitors. J Clin Oncol 28(36):5321–5326. doi:10.1200/JCO.2010.27.9943

26. Margolin AA, Nemenman I, Basso K, Wiggins C, Stolovitzky G, Dalla Favera R, Califano A (2006) ARACNE: an algorithm for the reconstruction of gene regulatory networks in a mammalian cellular context. BMC Bioinformatics 7(Suppl 1):S7. doi:10.1186/1471-2105-7-S1-S7

27. Margolin AA, Wang K, Lim WK, Kustagi M, Nemenman I, Califano A (2006) Reverse engineering cellular networks. Nat Protoc 1(2):662–671. doi:10.1038/nprot.2006.106

28. Murphy DM, Buckley PG, Bryan K, Watters KM, Koster J, van Sluis P, Molenaar J, Versteeg R, Stallings RL (2011) Dissection of the oncogenic MYCN transcriptional network reveals a large set of clinically relevant cell cycle genes as drivers of neuroblastoma tumorigenesis. Mol Carcinog 50(6):403–411. doi:10.1002/mc.20722

29. Northcott PA, Fernandez LA, Hagan JP, Ellison DW, Grajkowska W, Gillespie Y, Grundy R, Van Meter T, Rutka JT, Croce CM, Kenney AM, Taylor MD (2009) The miR-17/92 polycistron is up-regulated in sonic hedgehog-driven medulloblastomas and induced by N-myc in sonic hedgehog-treated cerebellar neural precursors. Cancer Res 69(8):3249–3255. doi:10.1158/0008-5472.CAN-08-4710

30. Northcott PA, Korshunov A, Witt H, Hielscher T, Eberhart CG, Mack S, Bouffet E, Clifford SC, Hawkins CE, French P, Rutka JT, Pfister S, Taylor MD (2011) Medulloblastoma comprises four distinct molecular variants. J Clin Oncol 29(11):1408–1414. doi:10.1200/JCO.2009.27.4324

31. Northcott PA, Rutka JT, Taylor MD (2010) Genomics of medulloblastoma: from Giemsa-banding to next-generation sequencing in 20 years. Neurosurg Focus 28(1):E6. doi:10.3171/2009.10.FOCUS09218

32. Oliver TG, Grasfeder LL, Carroll AL, Kaiser C, Gillingham CL, Lin SM, Wickramasinghe R, Scott MP, Wechsler-Reya RJ (2003) Transcriptional profiling of the Sonic hedgehog response: a critical role for N-myc in proliferation of neuronal precursors. Proc Natl Acad Sci USA 100(12):7331–7336. doi:10.1073/pnas.0832317100

33. Pession A, Tonelli R (2005) The MYCN oncogene as a specific and selective drug target for peripheral and central nervous system tumors. Curr Cancer Drug Targets 5(4):273–283

34. Pfaff E, Remke M, Sturm D, Benner A, Witt H, Milde T, von Bueren AO, Wittmann A, Schottler A, Jorch N, Graf N, Kulozik AE, Witt O, Scheurlen W, von Deimling A, Rutkowski S, Taylor MD, Tabori U, Lichter P, Korshunov A, Pfister SM (2010) TP53 mutation is frequently associated with CTNNB1 mutation or MYCN amplification and is compatible with long-term survival in medulloblastoma. J Clin Oncol 28(35):5188–5196. doi:10.1200/JCO.2010.31.1670

35. Pfister S, Remke M, Benner A, Mendrzyk F, Toedt G, Felsberg J, Wittmann A, Devens F, Gerber NU, Joos S, Kulozik A, Reifenberger G, Rutkowski S, Wiestler OD, Radlwimmer B, Scheurlen W, Lichter P, Korshunov A (2009) Outcome prediction in pediatric medulloblastoma based on DNA copy-number aberrations of chromosomes 6q and 17q and the MYC and MYCN loci. J Clin Oncol 27(10):1627–1636. doi:10.1200/JCO.2008.17.9432

36. Pfister SM, Korshunov A, Kool M, Hasselblatt M, Eberhart C, Taylor MD (2010) Molecular diagnostics of CNS embryonal tumors. Acta Neuropathol 120(5):553–566. doi:10.1007/s00401-010-0751-5

37. Pomeroy SL, Tamayo P, Gaasenbeek M, Sturla LM, Angelo M, McLaughlin ME, Kim JY, Goumnerova LC, Black PM, Lau C, Allen JC, Zagzag D, Olson JM, Curran T, Wetmore C, Biegel JA, Poggio T, Mukherjee S, Rifkin R, Califano A, Stolovitzky G, Louis DN, Mesirov JP, Lander ES, Golub TR (2002) Prediction of central nervous system embryonal tumour outcome based on gene expression. Nature 415(6870):436–442. doi:10.1038/415436a

38. Qi Q, Zhao Y, Li M, Simon R (2009) Non-negative matrix factorization of gene expression profiles: a plug-in for BRB-ArrayTools. Bioinformatics 25(4):545–547. doi:10.1093/bioinformatics/btp009

39. Remke M, Hielscher T, Korshunov A, Northcott PA, Bender S, Kool M, Westermann F, Benner A, Cin H, Ryzhova M, Sturm D, Witt H, Haag D, Toedt G, Wittmann A, Schottler A, von Bueren AO, von Deimling A, Rutkowski S, Scheurlen W, Kulozik AE, Taylor MD, Lichter P, Pfister SM (2011) FSTL5 is a marker of poor prognosis in non-WNT/non-SHH medulloblastoma. J Clin Oncol 29(29):3852–3861. doi:10.1200/JCO.2011.36.2798

40. Remke M, Hielscher T, Northcott PA, Witt H, Ryzhova M, Wittmann A, Benner A, von Deimling A, Scheurlen W, Perry A, Croul S, Kulozik AE, Lichter P, Taylor MD, Pfister SM, Korshunov A (2011) Adult medulloblastoma comprises three major molecular variants. J Clin Oncol 29(19):2717–2723. doi:10.1200/JCO.2011.34.9373

41. Rutkowski S, von Bueren A, von Hoff K, Hartmann W, Shalaby T, Deinlein F, Warmuth-Metz M, Soerensen N, Emser A, Bode U, Mittler U, Urban C, Benesch M, Kortmann RD, Schlegel PG, Kuehl J, Pietsch T, Grotzer M (2007) Prognostic relevance of clinical and biological risk factors in childhood medulloblastoma: results of patients treated in the prospective multicenter trial HIT'91. Clin Cancer Res 13(9):2651–2657. doi:10.1158/1078-0432.CCR-06-1779

42. Schwab M, Westermann F, Hero B, Berthold F (2003) Neuroblastoma: biology and molecular and chromosomal pathology. Lancet Oncol 4(8):472–480 (S1470204503011665[pii])

43. Scott DK, Straughton D, Cole M, Bailey S, Ellison DW, Clifford SC (2006) Identification and analysis of tumor suppressor loci at chromosome 10q23.3-10q25.3 in medulloblastoma. Cell Cycle 5(20):2381–2389 (3360[pii])

44. Suzuki R, Shimodaira H (2006) Pvclust: an R package for assessing the uncertainty in hierarchical clustering. Bioinformatics 22(12):1540–1542. doi:10.1093/bioinformatics/btl117

45. Swartling FJ, Grimmer MR, Hackett CS, Northcott PA, Fan QW, Goldenberg DD, Lau J, Masic S, Nguyen K, Yakovenko S, Zhe XN, Gilmer HC, Collins R, Nagaoka M, Phillips JJ, Jenkins RB, Tihan T, Vandenberg SR, James CD, Tanaka K, Taylor MD, Weiss WA, Chesler L (2010) Pleiotropic role for MYCN in medulloblastoma. Genes Dev 24(10):1059–1072. doi:10.1101/gad.1907510

46. Taylor RE, Bailey CC, Robinson KJ, Weston CL, Walker DA, Ellison D, Ironside J, Pizer BL, Lashford LS (2005) Outcome for patients with metastatic (M2–3) medulloblastoma treated with SIOP/UKCCSG PNET-3 chemotherapy. Eur J Cancer 41(5):727–734. doi:10.1016/j.ejca.2004.12.017

47. Westermann F, Muth D, Benner A, Bauer T, Henrich KO, Oberthuer A, Brors B, Beissbarth T, Vandesompele J, Pattyn F, Hero B, Konig R, Fischer M, Schwab M (2008) Distinct transcriptional MYCN/c-MYC activities are associated with spontaneous regression or malignant progression in neuroblastomas. Genome Biol 9(10):R150. doi:10.1186/gb-2008-9-10-r150

48. Zitterbart K, Filkova H, Tomasikova L, Necesalova E, Zambo I, Kantorova D, Slamova I, Vranova V, Zezulkova D, Pesakova M, Pavelka Z, Veselska R, Kuglik P, Sterba J (2010) Low-level copy number changes of MYC genes have a prognostic impact in medulloblastoma. J Neurooncol 102:25–33. doi:10.1007/s11060-010-0289-3